The Missing Link in the Magnetism of Hybrid Cobalt Layered Hydroxides: The Odd–Even Effect of the Organic Spacer

Dr. Víctor Oestreicher, Dr. Diego Hunt, Dr. Christian Dolle, Paula Borovik, Prof. Matías Jobbágy, Dr. Gonzalo Abellán, Prof. Eugenio Coronado

In memory of Jesús Carnicer Murillo

Abstract

A dramatic change in the magnetic behaviour, which solely depends on the parity of the organic linker molecules, has been found in a family of layered Co^{II} hydroxides covalently functionalized with dicarboxylic molecules. These layered hybrid materials have been synthesized at room temperature using a one-pot procedure through the *epoxide route*. While hybrids connected by odd alkyl chains exhibit coercive fields (H_c) below ca. 3500 Oe and show spontaneous magnetization at temperatures (T_M) below 20 K, hybrids functionalized with even alkyl chains behave as hard magnets with H_c>5500 Oe and display a T_M higher than 55 K. This intriguing behaviour was studied by density functional theory with the incorporation of a Hubbard term (DFT+U) calculations, unveiling the structural subtleties underlying this observation. Indeed, the different molecular orientation exhibited by the even/odd alkyl chains, and the orientation of the covalently linked carboxylic groups modify the intensity of the magnetic coupling of both octahedral and tetrahedral in-plane sublattices, thus strongly affecting the magnetic properties of the hybrid. These findings offer an outstanding level of tuning in the molecular design of hybrid magnetic materials based on layered hydroxides.

The hybrid approach has been widely used for the development and design of novel materials with tuneable chemical and physical properties at the nanoscale.[1-4] In this context, layered two-dimensional (2D) systems, especially those based on earth-abundant metals, are playing a key role, as they are often forming hybrid materials, which are convenient for a plethora of applications ranging from biomedicine, catalysis or magnetism, to energy storage and conversion.[5-12] Among others, layered hydroxides stand out due to their unparalleled chemical versatility which allows a precise control of their composition at the atomic or molecular level.[13]

Layered double hydroxides (LDHs) take a special role in the layered hydroxide family as they exhibit purely electrostatic interactions between the layers and the intercalated anions. These lamellar systems display *hydrotalcite*-like structures composed of positive charged sheets where both constituent M^{II} and M^{III} octahedral cations can be tuned.[14] Concerning magnetism, their rational modification permits the modulation of the nature of the intralayer coupling, ranging from antiferro- (AF) to ferromagnetic (F);[15] however, the interlayer coupling mainly depends on the dipolar interactions, promoting AF behaviour at wide basal space distances (d_{BS}). These systems usually show spontaneous magnetization

below a certain temperature, T_M, which is lower than ca. 15 K. Still, the influence of the interlamellar spacing on the magnetic properties has shown to be very limited, with only subtle modifications by different d_{BS},[16] or complex multistep covalent functionalization.[17] This may be due to the electrostatic nature of the interaction between the magnetic layers and the organic spacers.

An interesting route to overcome this limitation is to move from electrostatic to covalent interactions. Along this front, *α*-Co^{II} hydroxides (or *simonkolleite*-like structures) are optimal candidates since they can be considered as already naturally-occurring covalently functionalized layered hydroxides.[18] They show two distinguishable coordination environments, namely octahedral centers—$Co^{II}(O_h)$—within the layers (as in the case of LDHs) and tetrahedral sites—$Co^{II}(T_d)$—located at the basal planes with 3 OH- functionalities. The fourth position within this tetrahedral environment can be used for grafting different inorganic or organic species (Scheme **1**). Upon functionalization, the electronic and magnetic properties are thus tuneable by changing both the grafted (covalent) ligand and the $Co^{II}(T_d)$ ratio, resulting in more conductive systems with higher T_M values (from 30 to 55 K) in comparison to LDHs.[19-24] In particular, the covalent functionalization with organic species, such as aliphatic or aromatic carboxylic and dicarboxylic acids has been widely explored to enlarge the interlayer distance and thus promote a change in the magnetic behaviour. Curiously, with alkyl chains this research has been restricted to the study of hybrids containing even numbers of carbon atoms,[23] neglecting the hybrids containing odd-numbered alkyl chains, except in the case of Cu^{II} hydroxydicarboxylates.[24] In the case of Co^{II} hybrids, T_M values around 50 K have been reported that seem to be independent of the chemical and physical nature of the functionalization and the interlayer spacing.[5, 25]

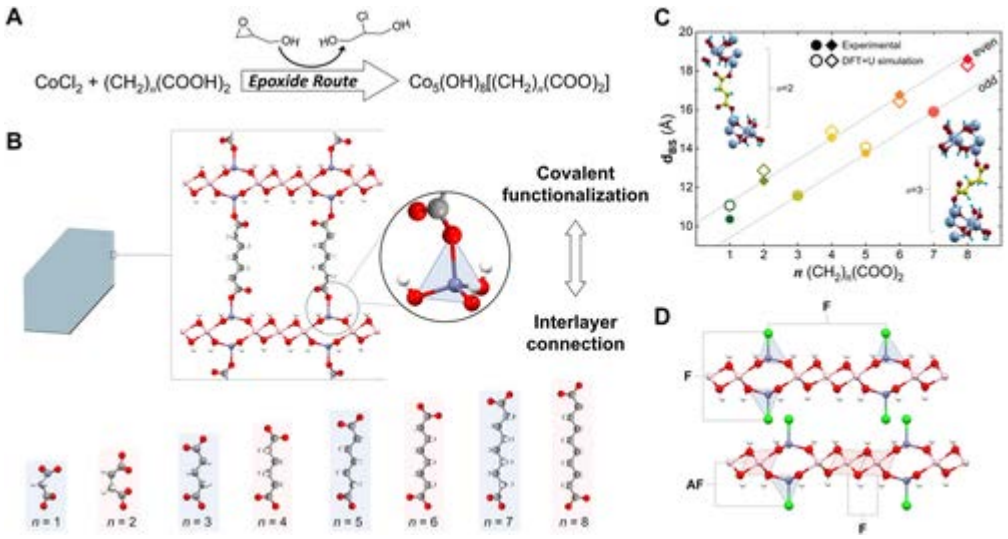

Scheme 1

(A) Synthesis of α-Co^{II} hydroxydicarboxylate structures driven by our one-pot room temperature method: the *epoxide route*. (B) The hybrid layered materials are based on *simonkolleite*-like layers (containing octahedral -in red- and tetrahedral -in blue- coordination for Co^{II}) bridged by dicarboxylic molecules (from malonic, *n*=1, to sebacic, *n*=8, acids) covalent functionalized through the tetrahedral Co^{II}. (C) Experimental (filled symbols) and DFT+U (open symbols) basal space distance (d_{BS}) as a function of the number of methylene groups (*n*), for odd

(circles) and even (diamond) members. (D) Intralayer magnetic coupling in α-Co^{II} hydroxychloride phase: anti- (AF) and ferromagnetic (F) coupling.

Taking advantage of the state of the art and our previous experimental and computational reports,[20, 26, 27] we conducted a thorough systematic study based on the microscopic understanding of α-Co^{II} hydroxydicarboxylate phases with interlayer functionalization ranging from malonic (*n*=1) to sebacic (*n*=8) acid. Expectedly, the even members depict a ferrimagnetic (FI) behaviour[21] with T_M>55 K while, to our surprise, the odd members show a distinctively lower T_M of ca. 20 K. This unexpected behaviour was rationalized on the basis of DFT+U simulations. Our results suggest that small molecular structural changes, such as the orientation of the organic linkers between the layers and the disposition of the carboxyl groups, result in sharply different magnetic behaviour of the layer itself, being the torsion of the covalently linked carboxylic groups the main responsible of change in coupling between both octahedral and tetrahedral sublattices within the layers. These novel structure–property outcome, missing for more than 20 years, paves the way towards the design of new hybrid functional materials where the overall magnetism is governed by something as subtle as the number of carbon atoms of the grafted molecules (i.e. molecular parity).

Generally, the synthesis of hybrid layered hydroxides requires hydrothermal conditions at elevated temperatures (100–250 °C) and a post recrystallization process for anion exchange.[5, 6] However, these time-consuming procedures do not guarantee obtaining of pure crystallographic phases.[28] Therefore, we decided to employ our *one-pot* room temperature method: the so-called *epoxide route* (Experimental Section in the Supporting Information).[29] This method has been successfully employed for the synthesis of several layered hydroxides,[20, 30] LDHs[31] and their hybrid forms,[32] MOFs based on Cu^{II} and carboxylic linkers,[33] and even gold nanoparticles.[34]

The syntheses were carried out at room temperature and, for the here presented layered hybrid materials, we obtained blue-greenish solids with the stoichiometric composition of $Co_5(OH)_8[(CH_2)_n(COO)_2]$. PXRD characterization (Figure S1) confirms the layered structures with typical (00*l*) reflections at lower *2-theta* values, associated with basal space distances (d_{BS}) ranging from ca. 10–19 Å. The (110) reflections, associated with the intralayer distance and centred at ca. 59°, remain practically unchanged for all hybrids (Figure S2). In contrast, the (00*l*) peaks for those samples connected by molecules with an even number of carbon atoms show a systematic shift towards lower *2-theta* values (higher d_{BS}), compared to the consecutive odd members, resembling a zigzag behaviour. At the same time, the PXRD peaks recorded from the even membered group are more intense and narrower (lower FWHM) compared to the odd members, pointing to larger crystal domains. The d_{BS} values can be plotted as a function of the number of methylene units (*n*), showing a zigzag behaviour of the BS (Scheme **1 C**), in concordance with previous reports for related phases of Cu^{II} and

Co^{II}.[23, 24] Interestingly, both sets of values (even and odd) can be fitted by two independent linear functions with an increment for d_{BS} of ca. 1.08 Å/CH_2. Nonetheless, the difference in the intercepting values deviates by more than 15 %, ranging from 8.33 Å to 10.17 Å for odd and even families, respectively. The structural changes observed by PXRD alerts about different dispositions of the organic moieties into the interlayer space that should depend on the parity of the dicarboxylate molecules (vide infra),[23] affecting both d_{BS} and the packing of the organic molecules, much like an arrangement of molecules in self-assembled monolayers.[35]

The presence of two coordination environments for Co^{II} were confirmed by UV/Vis diffuse reflectance spectroscopy (Figure S3). While the broad band centred ca. 500 nm is assigned to $Co^{II}(O_h)$, the strong band with twin-peaks at 592 nm and 637 nm is ascribable to $Co^{II}(T_d)$.[18, 20] The recorded blueshift of ca. 30 nm for the $Co^{II}(T_d)$ band in respect to α-Co^{II} hydroxychloride proofs the sensitivity of UV/Vis spectroscopy to distinguish crystallographic environments (Figure S4),[20] allowing to exclude the presence of hydroxychloride and/or Co^{III} phases.[36]

Attenuated total reflectance Fourier-transform infrared spectroscopy (ATR-FTIR) was used to confirm the incorporation of the dicarboxylic molecules into the hybrids (Figure S5). Two bands at ca. 2925–2850 cm^{-1} can be attributed to asymmetric and symmetric CH_2 stretching vibrations. Their intensity increases with the length of the molecule.[16, 37, 38] The strong bands at ca. 1750–1250 cm^{-1} are assigned to asymmetric and symmetric stretching modes of the carboxylic groups.[39] The higher intensity of the asymmetric band with respect to the symmetric one, and the corresponding difference $\Delta\nu=\nu_{asym}-\nu_{sym}$ of more than 100 cm^{-1}, suggest an unidentate coordination (Scheme **1 B**).[40] Notably, a zigzag behaviour in $\Delta\nu$ values of around 17 % for odd-even groups was observed (Figure S6), where the main responsible contribution for this shift is associated with the asymmetric band (ca. 25 cm^{-1}). Considering that the asymmetric and symmetric vibrational frequencies in unidentate carboxylates are closer to the vibrations of C=O (≈1700 cm^{-1}) and C-O (≈1400 cm^{-1}) in the carboxylic acid form,[41] this behaviour can be associated with a different disposition of the carboxylic groups. Finally, the broad band centred at ca. 3450 cm^{-1} is attributed to the presence of interlayer water molecules (O−H stretching modes),[39] and the bands below 1000 cm^{-1} are related to Co−O stretching and Co−OH bending vibrations.[28]

Field emission scanning electron microscopy confirms for all cases a flower-like morphology with similar micrometric sizes comprised between 1–5 µm (Figure S7).

To gain further information regarding the thermal stability of the hybrid phases, TGA measurements were performed. The thermal decomposition was followed under oxidizing conditions at 5 °C min^{-1} (Figure S8, Table S1); all samples show two main weight loss steps. While the first step below 100 °C is attributed to the loss of both physisorbed and interlayer water,[13] the second one, at ca. 210 °C, is ascribed to the decomposition of the organic molecules and the dehydroxylation of structural OH groups, resulting in a collapse of the layered structure.[18] This collapse takes place ca. 75 °C below the

thermal decomposition of α-Co^{II} hydroxychlorides,[25] confirming the dependence of the thermal stability caused by the interlayer functionalization.[13] Finally, in combination with elemental analysis and EDS measurements (no traces of Cl were observable), the degree of functionalization was estimated to be 39–40 %, the highest value imposed by the *Simonkolleite* structure (Table S2 and S3).[42] To summarize, the establishment of layered structures showing covalent attachment of dicarboxylic molecules with varying chain length to the tetrahedrally coordinated Co metals, in the form of $Co_5(OH)_8[(CH_2)_n(COO)_2]$ can be safely concluded.

Regarding the magnetism of these materials, the intralayer coupling is governed by F interactions between Co in identical coordination environments (O_h-O_h and T_d-T_d) and AF between the coordination in different environments (O_h-T_d), showing locally uncompensated moments resulting in layers that behave as ferrimagnets.[20, 21] In addition, the interlayer coupling and the overall magnetism can be tuned by solely changing the $Co^{II}(T_d)$ ratio (Scheme **1 D**).[20, 21] In our study, the $Co^{II}(T_d)$ and $Co^{II}(O_h)$ population remains constant for all the family, with the parity of the organic anion between layers being the only parameter that can be modified.

The magnetic experimental results are summarized in Figure S8–S15 and Table S4. Remarkably, the α-Co^{II} hydroxydicarboxylate family exhibits clearly distinct behaviours that can be divided into two groups, depending on the parity of the organic molecule, exclusively. At first glimpse, the even members present magnetization temperatures (T_M, defined as the point in which $\chi''_M \neq 0$) higher than 55 K and coercive fields higher than 5.5 kOe, as expected according to previous reports.[19, 22, 23] However, the odd members, never reported before, show an unexpected lower T_M of around 20 K and coercive fields lower than 3.5 kOe. To highlight the different magnetic behaviour between odd and even functionalization, Figure **1** compiles the macroscopic magnetic characterization of *n*=4 (in red: A–D) and *n*=5 (in blue, E–H) as representative members of the even and odd α-Co^{II} hydroxydicarboxylate families (the other members of the family can be found in Figure S8–S15).

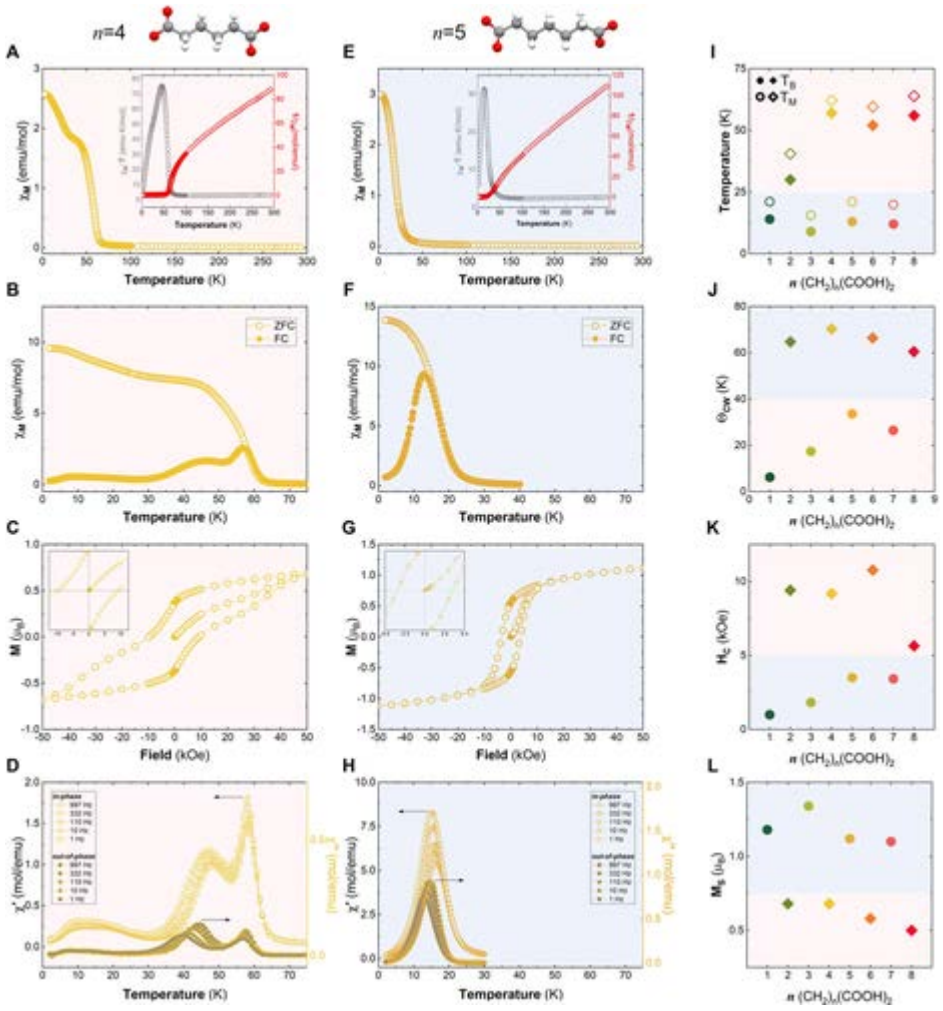

Figure 1

Magnetic characterization for samples *n*=4 (left in red) and *n*=5 (middle in blue) containing adipic and pimelic acid, respectively. Magnetic susceptibility as a function of temperature (χ_M vs. T) with an external applied field of 1000 Oe, where the inset represents the thermal dependence of χ_M·T and the fitting of the $1/\chi_M$ to a Curie–Weiss law (A and E). FC/ZFC with an external applied field of 100 Oe (B and F). Hysteresis cycle at 2 K, where the inset depicts the low field region (C and G). Thermal dependence of dynamic susceptibility for the in-phase (χ_M') and the out-of-phase (χ_M'') signals at 1, 10, 110, 332 and 997 Hz (D and H). The right panel depict the zigzag behaviour of the representative magnetic parameters for odd (circles) and even (diamond) members: magnetization (opened symbols) and blocking (filled symbols) temperatures (I), Curie–Weiss temperature (J), coercive field (K) and saturation magnetization (L).

The DC susceptibility measurements (χ_M) exhibit a continuous increase upon cooling, with pronounced growth starting at 70 K vs. 30 K for *n*=4 and *n*=5 samples, respectively. Moreover, the χ_M·T product also increases exhibiting a sharp peak at 47 K vs. 14 K, for *n*=4 and *n*=5 samples, respectively (Figures **1 A** and E and insets). Additionally, the temperature-independent component in χ_M·T confirms the absence of extrinsic magnetic impurities such as Co^{III} spinels, emphasizing the phase purity of the whole family.[38, 43] Spontaneous magnetization is confirmed by the strong increase of DC magnetization (Figures

1 B and F) and by a peak in the in-phase and out-of-phase components observed in the dynamic AC susceptibility measurements, with values of T_M=62 K for *n*=4 and T_M=21 K for *n*=5, respectively (Figures **1 D** and H). The strong frequency dependence observed in the dynamic susceptibility suggests a spin glass-like behaviour, as reported for α-Co^{II} hydroxyhalide compounds,[20] which can be attributed to the presence of different sublattices or microdomains.[21] Hysteresis loops recorded at 2 K further confirm the spontaneous magnetization for both samples, where large spin–orbit coupling is evidenced by the magnitude of the coercive field (Figures **1 C** and G).[22] In addition, Figure **1 I**–L summarize representative magnetic parameters in which the overall magnetic behaviour can be divided in two distinct groups, the even (highlighted in red) and odd (blue) members. Both magnetization and blocking temperature extracted from field cooled/zero-field cooled (FC/ZFC) experiments switch from values lower than 25 K for odd members to values around 50 K for even ones, alerting about strong differences on the magnetic coupling nature (Figure **1 I**). To gain deeper insights into the magnetic behaviour of this family, the inverse of the magnetic susceptibility (1/χ) can be fitted according to a Curie–Weiss law in the 200–300 K region. Figure **1 J** compiles the θ_{CW} (C parameters in Table S4). Once again, the difference between even and odd members is striking, as the even members present θ_{CW} values around 66 K while the odd ones depict ca. 21 K, almost three times smaller. Finally, Figures **1 K** and L depicts a switching of coercive field and the saturation values, respectively, depending on the parity of *n*, exclusively. The difference between the experimental value and the M_{sat}, estimated by employing a Néel model, can be attributed to the complex magnetic structure of this type of compounds.[30]

Indeed, the observed changes in the magnetism cannot be explained by changes in the $Co^{II}(T_d)$ ratio, according to previous reports for α-Co^{II} hydroxychloride[21] and α-Co^{II} hydroxyhalides.[20] Additionally, the observed anomalous switching in the magnetic coupling, which is strongly dependent on the number of carbon atoms, cannot solely be explained based on d_{BS} enhancement or dipolar interactions.[5, 6, 25] The changes in the magnetic nature of the layers must be related with the different orientation and/or the torsion of the organic molecules that modify the coupling among both sublattices (O_h and T_d), where the covalent functionalization with bridging molecules must play a unique role. Hence, to elucidate the origins of this atypical magnetic behaviour, we carried out a thorough study employing first principles calculations based on density functional theory (DFT).

It is well known that DFT underestimates the barriers of chemical reactions, the band gaps of materials, and charge transfer excitation energies; all these limitations concerning to charge delocalization.[44] To solve that, in our calculations, the incorporation of a Hubbard term (DFT+U) in the Kohn–Sham Hamiltonian that penalizes on-site electron interactions and inhibits *d*-charge delocalization was taken into account, given that it has proven effective to correct the well-known DFT deficiencies to describe the electronic properties of transition metal oxides.[45-47] The understanding of structural and electronic properties in Co-based hydroxylated phases by DFT+U simulation hereby requires an optimized Hubbard parameter (U), as we previously demonstrated.[20, 26, 27] Hence, in order to understand this complex

magnetic behaviour, a detailed analysis of the structure was carried out. It is important to note that in all calculations no symmetry restrictions were imposed on atomic relaxations; and in addition, different initial conditions were evaluated to ensure the ground state of the system. In addition, different distributions of Co^{Td} sites were explored in order to evaluate the unlike possibility of having Co^{Td}–Co^{Td} clustering (Figure S16).

After performing atomic relaxations, the optimized structures can successfully explain the experimentally observed zigzag behaviour in d_{BS} values (Scheme **1 C**). In addition, differences in the orientation of almost 30° (Figure **2 A**) for the molecules in the interlayer space are observed. The even molecules adopt an almost orthogonal disposition with respect to the individual sheets, $\alpha_{\perp} \simeq 85°$, resulting in larger d_{BS}; while the odd ones are significantly tilted, $\alpha_{\perp} \simeq 56°$ (Figure **2 B**). Besides the orientation of the molecules, a marked change in the disposition of the carboxyl groups is observed (Scheme **1 C** and Figure **2 A**). In the case of the even ones, both dipoles are pointing towards the layers and to the same side, while in the odd ones the dipoles are parallel to the layer and in different direction (Figure **2 A** and inset). Hence, significant torsions in the aliphatic chains that resemble helicoidal structures are noticeable, resulting in a remarkable switching in the optimized distance of the covalent bonding, Co^{Td}–O_{COO} (from ca. 1.96 Å [*n*=5] to 2.04 Å [*n*=4]; Figure **2 C** and Table S5). Therefore, this fact, in addition to the changes in the disposition of the carboxylic group, seem to be the underlying reason behind the differences in the intralayer coupling between the Co atoms resulting in such dramatic change in the magnetic behaviour. Indeed, for related azobenzene LDH hybrid systems based on electrostatic interactions, the tension induced by *cis*–*trans* isomerization triggers a compression/modification of the in-plane structure resulting in subtle modifications on the magnetic properties (e.g. T_M variation of ca. 1 K).[48] The same applies to thermoresponsive azocompounds showing slight changes in the basal space upon switching,[49] or to structurally distorted flower-like magnetic LDHs.[50]

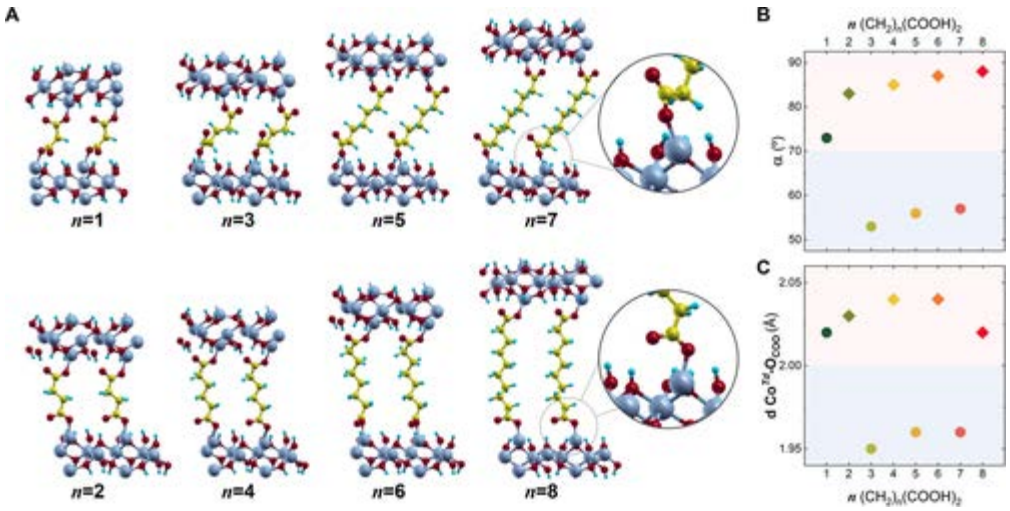

Figure 2

Optimized structures for Co_3^{Oh} Co_2^{Td} $(OH)_8[(CH_2)_n(COO)_2]$ supercells with *n* ranging from n_{DFT+U}=1 to n_{DFT+U}=8 (A). Estimated parameter for optimized supercells such as angle between the functionalization and the layer (α) (B) and Co^{Td}–O_{COO} bond lengths (C) as a function of *n*.

In this sense, the influence on the magnetic properties of the torsion in the Co^{Td}–O_{COO} bonds will be presumably more acute. In order to prove this hypothesis, we designed a control experiment in which both odd and even interlayer anions are connected only by one extreme (i.e. α-Co^{II} hydroxycarboxilate, $Co_5(OH)_8[CH_3(CH_2)_m(COO)]_2$ with monocarboxylic molecules. See Figure S17-19), thus minimizing torsion.

DFT+U calculations corroborates the absence of torsion showing angles and Co^{Td}–O_{COO} bond distances similar to even molecules connected by both extremes, for example, dicarboxylic molecules (Figure **3**, Figure S20 and Table S6).

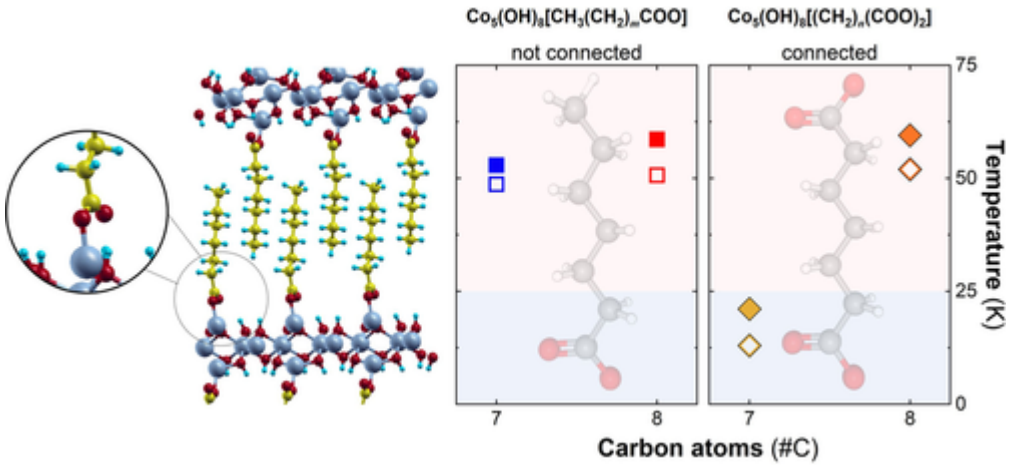

Figure 3

Optimized structure for α-Co^{II} hydroxycarboxilate supercells with heptanoate (#C=7). The inset shows the same disposition of carboxylic groups respect to the layer as in the case of the even dicarboxylic molecules. Magnetic

parameters such as blocking (opened symbols) and magnetization (filled symbols) as a function of the number of carbon atoms in the functionalized molecules alert about the odd-even effect only when bridged dicarboxylic molecules (connected) are employed.

Furthermore, magnetic measurements confirm our assumption since both monocarboxylated phases (heptanoate, #C=7, and octanoate, #C=8) exhibit almost identical behaviour independently of the nature of the parity of the molecule (see Figure S21 and Table S7).

Hence, these experiments clearly demonstrate that the odd-even effect solely takes place when bridging molecules as dicarboxylic acids are employed, as a consequence of the effect induced by torsions in the orientation of the carboxylic group and the Co^{Td}–O_{COO} distances. Thus, revealing the missing link in the magnetism of layered hydroxides.

In conclusion, we have demonstrated that the covalent functionalization of α-Co^{II} hydroxides with different dicarboxylate ligands induces tremendous changes in the magnetic behaviour, exclusively depending on the parity of the introduced dicarboxylic molecule. The unexpected behaviour of the hybrids functionalized with odd numbered chains, disregarded in the literature so far, opens the door for unprecedented level of tuning in the magnetism of layered hydroxides. This work illustrates how molecular engineering enables the straightforward synthesis of new multifunctional materials, with unparalleled control over their key properties.

Acknowledgements

This work was supported by the European Research Council (ERC Starting Grant No. 2D-PnictoChem 804110 to G.A. and ERC Advanced Grant Mol-2D 788222 to E.C.), the Spanish MICINN (PID2019-108643GA-I00 to G.A., Unit of Excellence "María de Maeztu" CEX2019-000919-M, and project MAT2017-89993-R co-financed by FEDER) and the Generalitat Valenciana (CIDEGENT/2018/001 to G.A., Prometeo/2017/066, and iDiFEDER/2018/061 co-financed by FEDER). D.H. acknowledge CONICET for financial support and CNEA Computing Clusters for computer time (density functional theory calculations). M.J. acknowledges UBACyT 20020130100610BA and CONICET PIP 11220170100991CO for financial support. The Ministry of Education and Science of Russian Federation (Agreement No.14.W03.31.0001) is gratefully acknowledged. Authors thanks to Dr. G. Agustí and Dr. J. M. Martínez for magnetic measurements. V.O. is member of ALN.

Conflict of interest

The authors declare no conflict of interest.

References

1. P. Gómez-Romero, C. Sanchez, *Functional Hybrid Materials*, Wiley, New York, 2005, pp. 1– 14.
2. L. Nicole, L. Rozes, C. Sanchez, *Adv. Mater.* 2010, 22, 3208– 3214.
3. L. Nicole, C. Laberty-Robert, L. Rozes, C. Sanchez, *Nanoscale* 2014, 6, 6267– 6292.
4. C. Taviot-Guého, V. Prévot, C. Forano, G. Renaudin, C. Mousty, F. Leroux, *Adv. Funct. Mater.* 2018, 28, 1703868.
5. G. Rogez, C. Massobrio, P. Rabu, M. Drillon, *Chem. Soc. Rev.* 2011, 40, 1031– 1058.
6. P. Rabu, E. Delahaye, G. Rogez, *Nanotechnol. Rev.* 2015, 4, 557– 580.
7. J. Azadmanjiri, J. Wang, C. C. Berndt, A. Yu, *J. Mater. Chem. A* 2018, 6, 3824– 3849.
8. R. Patel, J. Tae Park, M. Patel, J. Kumar Dash, E. Bhoje Gowd, R. Karpoormath, A. Mishra, J. Kwak, J. Hak Kim, *J. Mater. Chem. A* 2018, 6, 12– 29.
9. I. Roger, M. A. Shipman, M. D. Symes, *Nat. Rev. Chem.* 2017, 1, 1– 13.
10. C. Tan, X. Cao, X.-J. Wu, Q. He, J. Yang, X. Zhang, J. Chen, W. Zhao, S. Han, G.-H. Nam, M. Sindoro, H. Zhang, *Chem. Rev.* 2017, 117, 6225– 6331.
11. Y. Liu, N. O. Weiss, X. Duan, H.-C. Cheng, Y. Huang, X. Duan, *Nat. Rev. Mater.* 2016, 1, 16042.
12. W. Zhang, Q. Wang, Y. Chen, Z. Wang, A. T. S. Wee, *2D Mater.* 2016, 3, 022001.
13. Q. Wang, D. O'Hare, *Chem. Rev.* 2012, 112, 4124– 4155.
14. F. Li, X. Duan, *Layered Double Hydroxides* (Eds.: X. Duan, D. G. Evans), Springer, Berlin, 2006, pp. 193– 223.
15. G. Abellán, C. Martí-Gastaldo, A. Ribera, E. Coronado, *Acc. Chem. Res.* 2015, 48, 1601– 1611.
16. J. A. Carrasco, S. Cardona-Serra, J. M. Clemente-Juan, A. Gaita-Ariño, G. Abellán, E. Coronado, *Inorg. Chem.* 2018, 57, 2013– 2022.
17. J. A. Carrasco, A. Seijas-Da Silva, V. Oestreicher, J. Romero, B. G. Márkus, F. Simon, B. J. C. Vieira, J. C. Waerenborgh, G. Abellán, E. Coronado, *Chem. Eur. J.* 2020, 26, 6504– 6517.
18. R. Ma, Z. Liu, K. Takada, K. Fukuda, Y. Ebina, Y. Bando, T. Sasaki, *Inorg. Chem.* 2006, 45, 3964– 3969.
19. M. Kurmoo, *J. Mater. Chem.* 1999, 9, 2595– 2598.
20. V. Oestreicher, D. Hunt, R. Torres-Cavanillas, G. Abellán, D. A. Scherlis, M. Jobbágy, *Inorg. Chem.* 2019, 58, 9414– 9424.
21. J. R. Neilson, D. E. Morse, B. C. Melot, D. P. Shoemaker, J. A. Kurzman, R. Seshadri, *Phys. Rev. B* 2011, 83, 094418.
22. M. Kurmoo, *Chem. Mater.* 1999, 11, 3370– 3378.
23. M. Kurmoo, *Mol. Cryst. Liq. Cryst.* 2000, 341, 395– 406.
24. C. Hornick, P. Rabu, M. Drillon, *Polyhedron* 2000, 19, 259– 266.
25. M. Kurmoo, *Chem. Soc. Rev.* 2009, 38, 1353– 1379.
26. D. Hunt, G. Garbarino, J. A. Rodríguez-Velamazán, V. Ferrari, M. Jobbagy, D. A. Scherlis, *Phys. Chem. Chem. Phys.* 2016, 18, 30407– 30414.
27. D. Hunt, M. Jobbagy, D. A. Scherlis, *Inorg. Chem.* 2018, 57, 4989– 4996.
28. Z. Liu, R. Ma, M. Osada, K. Takada, T. Sasaki, *J. Am. Chem. Soc.* 2005, 127, 13869– 13874.

29. V. Oestreicher, M. Jobbágy, *Langmuir* 2013, 29, 12104– 12109.
30. N. Arencibia, V. Oestreicher, F. A. Viva, M. Jobbágy, *RSC Adv.* 2017, 7, 5595– 5600.
31. V. Oestreicher, I. Fábregas, M. Jobbágy, *J. Phys. Chem. C* 2014, 118, 30274– 30281.
32. V. Oestreicher, M. Jobbágy, *Chem. Eur. J.* 2019, 25, 12611– 12619.
33. V. Oestreicher, M. Jobbágy, *Chem. Commun.* 2017, 53, 3466– 3468.
34. V. Oestreicher, C. Huck-Iriart, G. Soler-Illia, P. C. Angelomé, M. Jobbágy, *Chem. Eur. J.* 2020, 26, 3157– 3165.
35. F. Tao, S. L. Bernasek, *Chem. Rev.* 2007, 107, 1408– 1453.
36. F. Leroux, E. M. Moujahid, C. Taviot-Guého, J.-P. Besse, *Solid State Sci.* 2001, 3, 81– 92.
37. J. A. Carrasco, R. Sanchis-Gual, A. S.-D. Silva, G. Abellán, E. Coronado, *Chem. Mater.* 2019, 31, 6798– 6807.
38. A. Seijas-Da Silva, R. Sanchis-Gual, J. A. Carrasco, V. Oestreicher, G. Abellán, E. Coronado, *Batteries Supercaps* 2020, 3, 499– 509.
39. M. Shabanian, M. Hajibeygi, A. Raeisi, *Layered Double Hydroxide Polymer Nanocomposites* (Eds.: S. Thomas, S. Daniel), Woodhead Publishing, Sawston, 2020, pp. 77– 101.
40. R. C. Mehrotra, R. Bohra, *Metal Carboxylates*, Academic Press, New York.
41. Y. Lu, J. D. Miller, *J. Colloid Interface Sci.* 2002, 256, 41– 52.
42. J. R. Neilson, J. A. Kurzman, R. Seshadri, D. E. Morse, *Chem. Eur. J.* 2010, 16, 9998– 10006.
43. G. Abellán, J. A. Carrasco, E. Coronado, *Inorg. Chem.* 2013, 52, 7828– 7830.
44. A. J. Cohen, P. Mori-Sánchez, W. Yang, *Science* 2008, 321, 792– 794.
45. B. Himmetoglu, A. Floris, S. de Gironcoli, M. Cococcioni, *Int. J. Quantum Chem.* 2014, 114, 14– 49.
46. C. Freysoldt, B. Grabowski, T. Hickel, J. Neugebauer, G. Kresse, A. Janotti, C. G. Van de Walle, *Rev. Mod. Phys.* 2014, 86, 253– 305.
47. H. J. Kulik, M. Cococcioni, D. A. Scherlis, N. Marzari, *Phys. Rev. Lett.* 2006, 97, 103001.
48. G. Abellán, E. Coronado, C. Martí-Gastaldo, A. Ribera, J. L. Jordá, H. García, *Adv. Mater.* 2014, 26, 4156– 4162.
49. G. Abellán, J. L. Jordá, P. Atienzar, M. Varela, M. Jaafar, J. Gómez-Herrero, F. Zamora, A. Ribera, H. García, E. Coronado, *Chem. Sci.* 2015, 6, 1949– 1958.
50. J. A. Carrasco, G. Abellán, E. Coronado, *J. Mater. Chem. C* 2018, 6, 1187– 1198.